



Nuclear microprobe analysis of ${}^7\text{Li}$ profile induced in HfB_2 by a neutron irradiation

D. Simeone ^{a,*}, X. Deschanel ^a, D. Gosset ^a, J.P. Bonal ^a, E. Berthoumieux ^b

^a Laboratoire d'Etude des Matériaux Absorbants, CEA, Ctr. d'Etude de Saclay, F 91191 Gif-sur-Yvette cedex, France

^b Laboratoire Pierre Sue, CEA, Ctr. d'Etude de Saclay, F 91191 Gif-sur-Yvette cedex, France

Received 18 February 1999; accepted 14 June 2001

Abstract

HfB_2 , a solid poor in boron, was irradiated by thermal neutrons in an experimental reactor. Using a nuclear microprobe, we have tracked lithium atoms produced by the ${}^{10}\text{B}(\text{n}, \alpha){}^7\text{Li}$ reaction and compared the calculated and measured ${}^7\text{Li}$ profiles in HfB_2 irradiated samples. This comparison shows that Li atoms do not diffuse during irradiation (323 K). The comparison of non-annealed and annealed irradiated HfB_2 plates clearly shows that lithium atoms do not migrate out of samples even at high temperatures (1273 K). These results associated to previous transmission electron microscopy (TEM) observations seem to show that lithium atoms are trapped by dislocation loops created by displacement cascades during neutron irradiation. © 2001 Elsevier Science B.V. All rights reserved.

1. Introduction

The family of boron solids possesses very particular and interesting structures. For example, many boron-rich solids, LaB_6 and B_4C , are based on 6-atom and 12-atom clusters forming unusual three-centre-bonds. The interest of such solids for the nuclear industry can be summarised by the fact that ${}^{10}\text{B}$ atoms capture neutrons according to the well-known ${}^{10}\text{B}(\text{n}, \alpha){}^7\text{Li}$ reaction. This reaction explains that boron solids are used to control and to shut down the power of nuclear plants.

A general goal of research on boron-rich solids is to acquire a better understanding of how their properties (species diffusion for instance) under neutron irradiation result from their distinctive structure and bonding. A previous work shows the evidence of lithium migration out of irradiated boron carbide [1]. Using the nuclear microprobe technique, it was possible to calculate a lithium diffusion coefficient in B_4C [2]. The aim of this

work is to study the Li diffusion in HfB_2 under neutron irradiation.

The space group of HfB_2 is $\text{P6}/\text{mmm}$ [3]. HfB_2 is composed of hexagonal unit cells, like AlB_2 . The cell parameters are, respectively, 3.14 and 3.47 Å. Fig. 1 presents a schematic diagram of the HfB_2 structure. In the boron sub-lattice, boron atoms are linked by sp^2 bonds [4]. The link between boron and hafnium atoms is due to a transfer of electrons from hafnium to boron atoms. The hafnium sub-lattice ensures a metal-like electrical behavior to HfB_2 .

In order to investigate a possible migration of ${}^7\text{Li}$ atoms out of the irradiated HfB_2 plates, we have measured the ${}^7\text{Li}$ concentration along the radius of the plates. This measurement has been performed using the nuclear reaction technique at microprobe facility of the Pierre Sue laboratory. In this work, we take advantage of the local sensitivity of the nuclear probe to localise lithium atoms on different HfB_2 plates irradiated and annealed at different temperatures. The comparison between the calculated and measured lithium profiles associated to previous data based on transmission electron microscopy (TEM) [5] observations leads us to propose a possible location for lithium atoms in the material.

* Corresponding author. Tel.: +33-1 69 08 29 20; fax: +33-1 69 08 90 82.

E-mail address: david.simeone@cea.fr (D. Simeone).

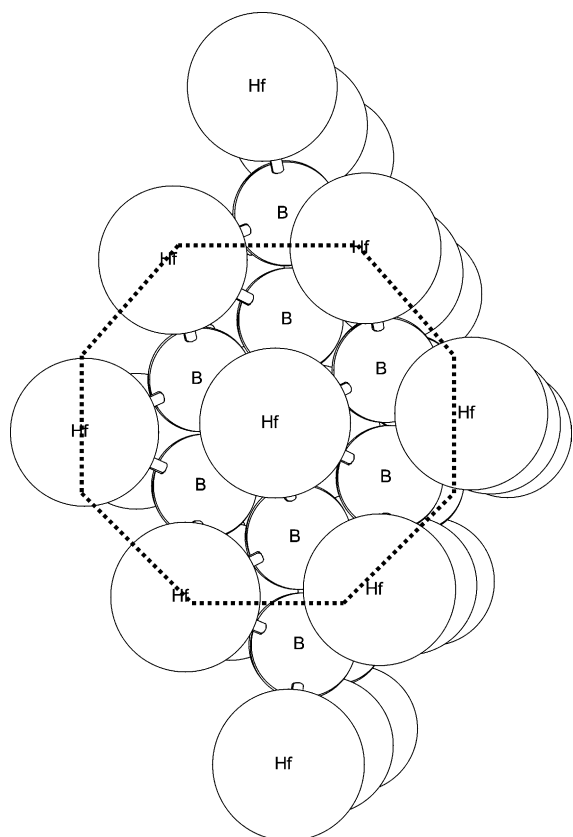


Fig. 1. Schematic description of HfB_2 unit cell; the dot line figures out the hexagonal basal plane.

2. Lithium production profile

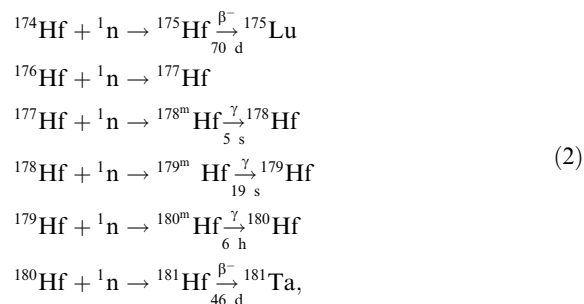
The high value of the $^{10}\text{B}(n, \alpha)^7\text{Li}$ reaction cross-section (3890 b for neutrons with a kinetic energy of 25 MeV) induces an important self-shielding effect along the thickness of the plate and modifies the ^{10}B distribution in the plate during the neutron irradiation. The

$^{10}\text{B}(n, \alpha)^7\text{Li}$ reaction cross-section can be described by the Breit Wigner formula [6]. ^{10}B atom is a light atom and no resonance exists for neutrons with kinetic energies up to 1 MeV, so that the $^{10}\text{B}(n, \alpha)^7\text{Li}$ cross-section follows a classical absorption law proportional to $(\sqrt{E})^{-1}$, where E is the neutron kinetic energy. The $^{10}\text{B}(n, \alpha)^7\text{Li}$ cross-section can be written as

$$\sigma(E) = A \sqrt{\frac{E_0}{E}}, \quad (1)$$

where $E_0 = 1$ MeV and $A = 0.606$ b.

Hafnium atoms also absorb neutrons according to the following reactions:



where m refers to unstable nuclei.

Table 1 presents the atomic fraction of different nuclei forming the samples, the microscopic absorption cross-section of different nuclei for thermal neutrons with a kinetic energy of 25 meV, and the macroscopic cross-section Σ used in our calculation. The comparison of the different Hf and ^{10}B macroscopic cross-sections clearly shows that the hafnium absorption can be neglected in the ^{10}B profile calculation. The ^7Li profiles have been calculated taking into account the effect of ^{10}B atoms only. In order to quantify the self-shielding effect induced by ^{10}B atoms in our samples, a form factor can be introduced. This form factor allows one to calculate the neutron flux depletion inside the material. This form factor can be expressed as follows:

Table 1

Atomic concentration, microscopic and macroscopic cross-sections of different nuclei in HfB_2 enriched at 90% in ^{10}B

Isotope	Microscopic cross-section for thermal neutrons (b)	Atomic fraction (%)	Macroscopic cross-section (cm^{-1})
^{10}B	3980	0.5999	
^{11}B	0	0.0666	
^{174}Hf	1500	0.0006	
^{176}Hf	15	0.0172	
^{177}Hf	380	0.0613	
^{178}Hf	75	0.0903	
^{179}Hf	65	0.0459	
^{180}Hf	14	0.1182	
^{10}B in the studied HfB_2 samples			244
Hf in the studied HfB_2 samples			3.5

$$f(x, E, t) = \left\{ \frac{\partial \Phi(\sigma, E, t)}{\partial E} \right\} / \left\{ \frac{\partial \Phi_{\text{up}}(\sigma, E, t)}{\partial E} \right\}, \quad (3)$$

where $\partial \Phi_{\text{up}}/\partial E$ is the neutron spectrum out of the HfB_2 sample, which is Maxwellian in our experiment. $f(x, E, t)$ can be expressed as the ‘optical’ path of neutrons in an infinite plate by the following formula:

$$f(x, E, t) = \frac{1}{4\pi} \int_0^{4\pi} \exp \left(- \int_0^1 N(P + \mu \mathbf{PM}, t) \times \sigma(E) \|\mathbf{PM}\| d\mu \right) d\Omega, \quad (4)$$

where x is the abscissa from the centre of the plate, N is the number of ^{10}B atoms at point M of the plate and P is a point at the surface of the plate.

After calculations, f can be written as

$$f(x, E, t) = \frac{1}{2} [E_2((LN_0^R(t) + xN_0^X(t))\sigma(E)) + E_2((LN_0^R - xN_0^X(t))\sigma(E))], \quad (5)$$

$$N_a^b(t) = \int_a^b N((a + \mu(b - a)), t) d\mu, \quad (6)$$

where $N_a^b(t)$ is the number of ^{10}B atoms along the path at the time t and E_2 is the exponential integral of the second order.

Then the number of ^{10}B atoms transmuted (i.e. of ^7Li atoms produced) is obtained by solving the following equation:

$$\frac{dN(x, t)}{dt} = -N(x, t) \int_0^\infty \frac{\partial \Phi_{\text{up}}(E)}{\partial E} f(x, t, E) \sigma(E) dE. \quad (7)$$

Fig. 2 shows the specific form of the form factor obtained at $t = 0$. A specific code has been developed to calculate the ^7Li profile along the reduced abscissa x/L for any neutron spectrum at any time.

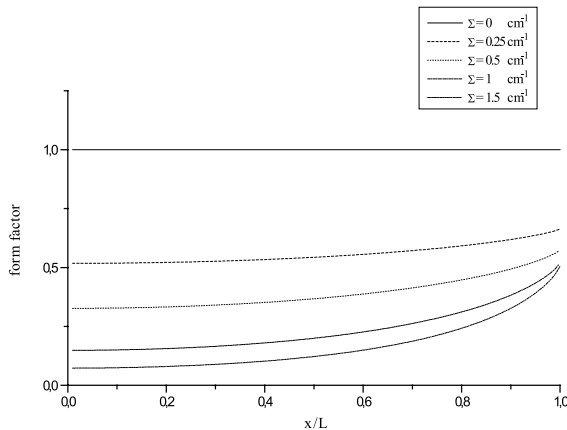


Fig. 2. Evolution of the form factor in HfB_2 as a function of the thickness for different macroscopic absorption cross-sections at the beginning of the neutron irradiation.

3. Experimental details

3.1. Samples preparation

Initial HfB_2 samples were elaborated with an initial ^{10}B isotopic composition $N(^{10}\text{B})/[N(^{10}\text{B}) + N(^{11}\text{B})]$ equal to 89.95% (at.) ($N(X)$ is the number of atoms of chemical element X per volume unit). The chemical composition of HfB_2 plates was in mass: 9.98% of boron, 89.12% of hafnium, 0.2% of carbon, 2700 ppm of Zr, 2200 ppm of W, 400 ppm of Fe, 4 ppm of Mg, 35 ppm of N, and 2330 ppm of O.

The plate density was 10.97 g/cm^3 (98% of the theoretical density). The average grain size was about $20 \mu\text{m}$.

For the microprobe analysis, a HfB_2 cylinder with a radius of 0.35 cm and a thickness of 0.15 cm has been irradiated. The pellet diameter is 4.6 times larger than the thickness, so that the pellet can be considered as an infinite plate. After irradiation, the cylinder was cut along the axial direction. Each half pellet was polished with an abrasive powder of $1 \mu\text{m}$ in grain size in order to obtain clean surfaces (cf. Fig. 3). Less than $5 \mu\text{m}$ of the surface was removed.

3.2. Sample irradiation

Samples were irradiated in quartz capsules filled with ^4He (0.5 bar), under a Maxwellian neutron flux. The value of the thermal neutron flux was about $2 \times 10^{14} \text{ n cm}^{-2} \text{ s}^{-1}$ and the irradiation time was 34.5 h.

Nuclear reactions producing tritium from ^7Li and ^{10}B atoms are threshold reactions. The threshold energy values for these reactions are 2.8 and 9.6 MeV, respectively [6]. Since in our experiments the neutron flux spectrum is Maxwellian, such nuclear reactions cannot

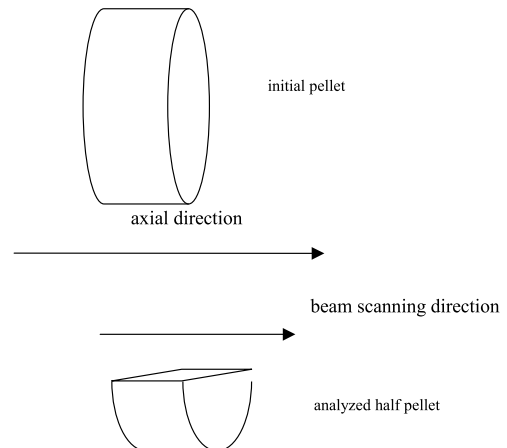


Fig. 3. Schematic description of the irradiated HfB_2 pellet analysed by the nuclear probe.

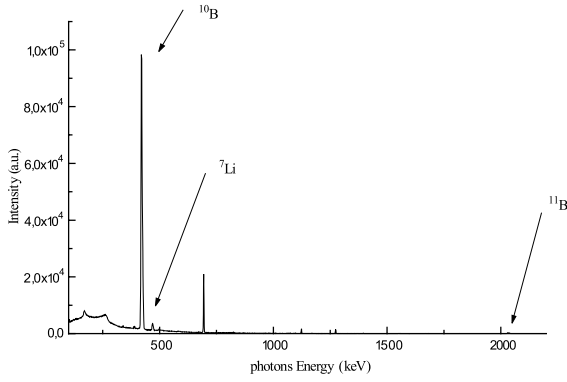
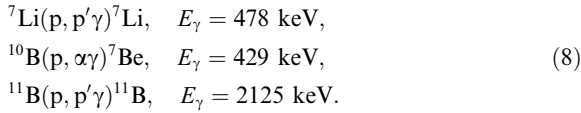


Fig. 4. Typical γ energy spectrum corresponding to the proton interaction with the samples. The three lines of interest are identified.

induce a diminution of the ${}^7\text{Li}$ concentration in the HfB_2 samples during the irradiation.

3.3. Microprobe experiment

The microprobe description is given in [1]. In the present work, ${}^7\text{Li}$ profiles have been measured by the following reactions:



The proton beam energy $E_p = 3.2$ MeV has been chosen to obtain accurate profiles along the plates in a reasonable time. Fig. 4 presents a typical photon energy spectrum corresponding to the proton interaction with the different elements (${}^{10}\text{B}$, ${}^{11}\text{B}$, ${}^7\text{Li}$) composing the samples.

4. Experimental results

The number of photons detected depends on the concentration of the analysed elements (${}^{10}\text{B}$, ${}^{11}\text{B}$, ${}^7\text{Li}$) according to the equation

$$N_j(\text{X}, x, t_m) = kN(\text{X}, x)N_p \int_{E_c}^{E_p} \frac{d^2\sigma}{d\Omega dE} \frac{dE}{dE/dx}, \quad (9)$$

where X is the element detected, N_j is the number of γ collected, x is the position of the proton spot in the material, k is a factor depending on the geometry and the detector efficiency, N_p is the number of incident protons, N is the number of element X per volume unit, $d^2\sigma/d\Omega dE$ is the cross-section for different reactions, dE/dx is the stopping power of the HfB_2 matrix described by Bethe's formalism and calculated according

to Ziegler and Biersack's [7] formulation and Bragg's rules [8].

A reliable standard of unirradiated HfB_2 is used to determine the initial ${}^{10}\text{B}$ concentration. Because there exists no reliable standard HfB_2 pellet including a known ${}^7\text{Li}$ concentration, the reference measurement of ${}^7\text{Li}$ concentration has been performed using a standard material (NBS) composed of Si (25 at.%), Ca (4.5 at.%), Na (9.4 at.%), O (61.1 at.%), and Li (500 at. ppm). Then the ${}^7\text{Li}$ concentration is obtained from (10) using the following equation:

$$\begin{aligned} N({}^7\text{Li}) &= N^{\text{NBS}}(\text{Li}) \frac{N_\gamma({}^7\text{Li})}{N_\gamma^{\text{NBS}}({}^7\text{Li})} \beta, \\ \beta &= \left\{ \int_{E_c}^{E_p} \frac{d^2\sigma}{d\Omega dE} \frac{dE}{\left(\frac{dE}{dx}\right)_{\text{NBS}}} \right\} / \left\{ \int_{E_c}^{E_p} \frac{d^2\sigma}{d\Omega dE} \frac{dE}{\left(\frac{dE}{dx}\right)_{\text{HfB}_2}} \right\}. \end{aligned} \quad (10)$$

The cut-off energy E_c of the ${}^7\text{Li}(p, p'\gamma){}^7\text{Li}$ reaction has been taken equal to 400 keV [9].

4.1. Effect of proton irradiation on irradiated HfB_2 samples

To avoid artefacts induced by the possible emission of photons by hafnium atoms irradiated by a proton beam, a hafnium sample was irradiated by a proton flux in the same condition as HfB_2 samples. No γ has been collected on the detector at 428, 478 and 2125 keV.

To separate photons induced by Hafnium activation under neutron irradiation (cf. Eq. (2)), we first collected γ spectra during the proton irradiation, and secondly, we collected γ emitted by samples after the proton beam was cut. The real γ spectrum is obtained by subtracting the two spectra.

4.2. Analysis of the different profiles

${}^{10}\text{B}$ profile. The short time of irradiation induced low variations in the ${}^{10}\text{B}$ concentration inside the different irradiated samples (about 8×10^{-3} in atomic concentration near the surface). Such a variation is not detectable by the nuclear microprobe technique and no ${}^{10}\text{B}$ profile could be obtained.

${}^7\text{Li}$ profile. Fig. 5 presents the ${}^7\text{Li}$ atoms profile as a function of the thickness in HfB_2 irradiated samples. The asymmetry of the ${}^7\text{Li}$ profile as a function of the thickness observed may be due to the fact that the neutron spectrum, which is more thermalised near the reflector, is not totally Maxwellian.

The comparison between calculated and measured profiles does not show the migration of ${}^7\text{Li}$ atoms out of the HfB_2 sample (Fig. 6). The average ${}^7\text{Li}$ atoms concentration measured by the nuclear microprobe technique (about $4.37 \pm 0.3 \times 10^{19}$ atoms cm^{-3}) agrees well

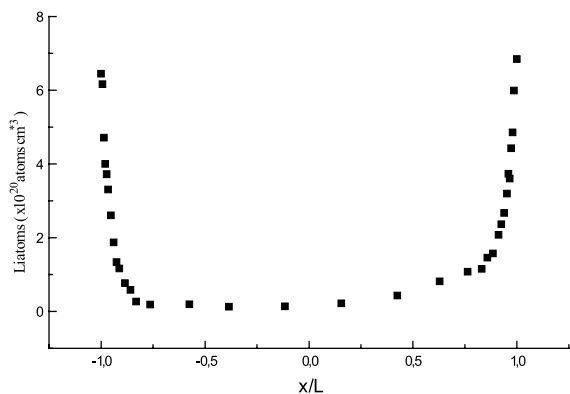


Fig. 5. Profile of ${}^7\text{Li}$ atoms in irradiated HfB_2 samples as a function of the thickness of the sample.

with that obtained by an ionic chromatography analysis (about $4.77 \pm 0.1 \times 10^{19}$ atoms cm^{-3}).

We have estimated the increase of temperature due to the ${}^{10}\text{B}(n, \alpha){}^7\text{Li}$ nuclear reaction heating during the neutron irradiation. For that, the temperature field is calculated using the well-known heat equation in the steady state case by the following equation:

$$T(x) = T_s + \frac{e^2}{4\lambda} \int_x^1 dy \int_0^y P(u) du, \quad (11)$$

where x and y are the reduced abscissa, e is the thickness of sample, T_s is the surface temperature of the pellet (323 K) and λ is the measured thermal conductivity of the unirradiated HfB_2 ($58 \text{ W m}^{-1} \text{ K}^{-1}$) and

$$P(x) = \frac{QdN(x, t)}{dx},$$

where Q is the transmutation energy (2.7 MeV/atom).

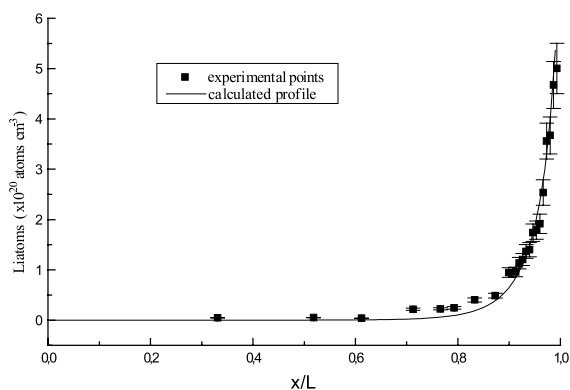


Fig. 6. Comparison between calculated and measured Li profile in HfB_2 irradiated samples.

The calculation of the temperature profile shows that the temperature can be considered as constant and equal to 323 K during the irradiation.

Fig. 6 shows that there is no migration of ${}^7\text{Li}$ atoms in irradiated HfB_2 samples for such a temperature. To study the possible migration of ${}^7\text{Li}$ atoms out of HfB_2 samples at higher temperatures, an irradiated HfB_2 sample has been annealed during 1 h at 1273 K under vacuum (the pressure was about 100 Pa) outside irradiation. Fig. 7 presents the comparison between the annealed and non-annealed HfB_2 irradiated samples. We observe a good agreement between the two profiles.

A difference between the profiles is observed near the reduced abscissa x/L equal to 0.8. This difference can be understood if we consider, as before, that the neutron spectrum is not really Maxwellian. The annealed sample irradiated near the reactor reflector was probably irradiated by a neutron spectrum more thermalised than the non-annealed sample. That is why fewer epithermal neutrons (with a kinetic energy of about 1 eV) were present in the annealed sample. This would explain the lower value of ${}^7\text{Li}$ concentration near 0.8 in the annealed sample.

The nuclear microprobe technique seems to show that at temperatures up to 1273 K, ${}^7\text{Li}$ atoms do not diffuse in irradiated HfB_2 samples for low neutron captures (5×10^{19} captures cm^{-3}).

From these studies (Figs. 6 and 7) we can deduce that lithium atoms may either stay in interstitial positions or produce lithium precipitates in the HfB_2 matrix. X-ray diffraction analysis have been done to detect lithium precipitates. The X-ray absorption coefficient of HfB_2 for $\text{CuK}\alpha 1$ radiation is equal to 1612 cm^{-1} . This implies that the probed depth is $6.2 \mu\text{m}$. In this area, the lithium concentration (at $x/L = 0.9$) is roughly equal to $6 \times 10^{20} \text{ cm}^{-3}$ (Fig. 6). This amount of Li is too small to create extra peaks on the X-ray diffraction diagrams. If periodic lithium precipitates produced under irradiation

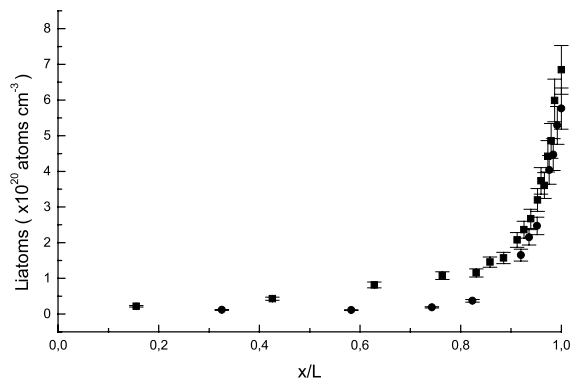


Fig. 7. Comparison between a HfB_2 annealed at 1273 K 1 h (dots) and non-annealed HfB_2 samples (squares) irradiated under neutron thermal flux.

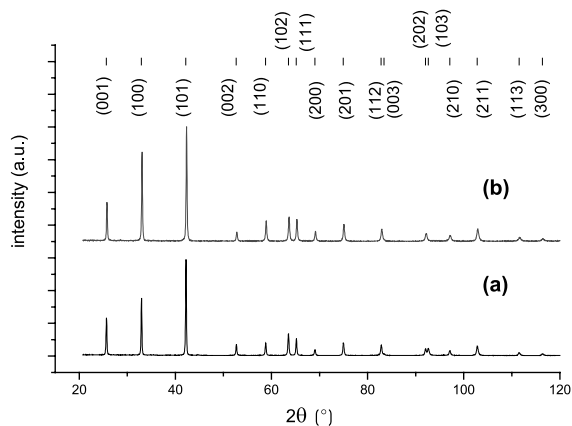


Fig. 8. Comparison of X-ray diffraction diagram on unirradiated (a) and irradiated (b). HfB_2 matrix. The lines above the graphs represent the calculated Bragg angles.

exist in the HfB_2 matrix, they should create a macroscopic strain field, associated to the variation of volume between the Li precipitates and the HfB_2 matrix, and a microscopic strain field associated to lattice parameters distortions of the HfB_2 matrix near precipitates. These two kinds of strains should induce a shift of the Bragg angles and a broadening of X-ray diffraction peaks in HfB_2 [10]. No measurable variations of the Bragg angles were measured on irradiated and annealed samples (Fig. 8). No differences can be seen on Hall Williamson plots between irradiated and unirradiated samples. Then, either a non-periodic network of Li precipitates are created or irradiation does not lead to the creation of Li precipitates. Previous TEM photographs had never shown any lithium precipitates in observed grains [5]. Therefore it seems that there are no lithium precipitates created by irradiation in the HfB_2 matrix.

5. Discussion

There are no data available on the diffusion of Li atoms in HfB_2 matrix. Therefore it has not been possible to estimate a diffusion coefficient of Li atoms at 1273 K ($0.34T_m$, where T_m is equal to 2653 K) but previous measurements [11] have shown the diffusion of lithium out of irradiated HfB_2 powder with a grain size of about $5 \mu\text{m}$ near 523 K ($0.19T_m$) during an annealing of 1 h. The atomic fraction of Li produced in their experiment was equal to 10% in HfB_2 matrix. X-ray diffraction diagrams showed clearly that the matrix was mainly amorphous at the end of the irradiation. The high concentration of Li and the amorphous character of the matrix can easily explain the diffusion of Li atoms out of grains in the powder. Then from this result, the annealing time and temperature chosen in our experiment

should allow the diffusion of lithium atoms out of HfB_2 slices. However, such a diffusion has clearly not been observed (Fig. 7) in our experiment.

No TEM observations of the microstructure were done on HfB_2 samples irradiated by thermal neutrons. However, TEM observations were done on HfB_2 samples irradiated by 550 keV He^+ ions at room temperature and annealed until 1873 K. These observations show that two different types of dislocation loops appear during an irradiation:

- Vacancy edge dislocation loops with a Burgers vector equal to $[0001]$. These loops lie in the (0001) plane.
- Interstitial loops in prismatic planes with a Burgers vector in the $(11\bar{2}0)$ direction.

After annealing at 1873 K, the density of vacancy loops remains constant and equal to $5 \times 10^{15} \text{cm}^{-3}$.

All these observations could explain the absence of lithium diffusion out of HfB_2 pellets irradiated by thermal neutrons. Vacancy loops created during the irradiation may trap lithium atoms in each HfB_2 grain. The motion of Li atoms may be blocked by dislocation loops and not diffuse out of the pellet even at high temperature explaining our experimental results.

6. Conclusion

The analyses of ^7Li concentration profiles in irradiated HfB_2 samples have clearly shown an absence of ^7Li migration in the samples for temperatures until 1273 K and low neutron capture numbers (5×10^{19} captures cm^{-3}). The X-ray diffraction analysis clearly shows neither any peaks broadening nor displacements of HfB_2 irradiated samples. This analysis of X-ray diffraction peaks on unirradiated and irradiated HfB_2 samples associated to TEM observations shows that no precipitate of lithium appears during irradiation. However, dislocation loops have been observed in irradiated HfB_2 pellets irradiated by He^+ ions with a kinetic energy of 550 keV using a TEM technique. This observation and ^7Li concentration measurements let us suppose that lithium atoms are trapped in grains by dislocation loops created by recoil nuclei damages during irradiation in the HfB_2 structure.

References

- [1] D. Simeone, X. Deschanel, B. Berthier, C. Tessier, J. Nucl. Mater. 245 (1997) 27.
- [2] X. Deschanel, D. Simeone, J.-P. Bonal, J. Nucl. Mater. 265 (1999) 321.
- [3] B. Post, F. Glaser, D. Moskovite, Acta Metall. 2 (1954) 20.
- [4] D. Greenwood, R. Parish, P. Thornton, Quaterly Rev. 20 (1966) 441.
- [5] P. Cheminant, thesis, Université d'Orsay, 1997.

- [6] D. Simeone, thesis, Université de Clermont-Ferrand, 1998.
- [7] J. Ziegler, Handbook of Stopping Power of Energetic Ions in All Elements, vol. 5, Pergamon, New York.
- [8] W. Bragg, R. Kleeman, *Philos. Mag.* 10 (1905) 5318.
- [9] R. Jarjis, PhD thesis, University of Manchester, 1979.
- [10] D. Simeone, D. Gosset, D. Quirion, X. Deschanel, *J. Nucl. Mater.* 264 (1999) 295.
- [11] W. Cummings, W. Clark, Radiation effects in Borides, GEAP-3749 Part III, 1962.